Published in final edited form as:
Chem Eng Sci. 2013 January 14; 85: 69–76. doi:10.1016/j.ces.2011.12.045.

Dispersion and Filtration of Carbon Nanotubes (CNTs) and Measurement of Nanoparticle Agglomerates in Diesel Exhaust

Jing Wang[1,2] and **David Y.H. Pui**[3]

[1]Institute of Environmental Engineering, ETH Zurich, 8093 Zurich, Switzerland [2]Empa, Analytical Chemistry, 8600 Dübendorf, Switzerland [3]Particle Technology Laboratory, University of Minnesota, 55414, USA

Abstract

Carbon nanotubes (CNTs) tend to form bundles due to their geometry and van der Walls forces, which usually complicates studies of the CNT properties. Dispersion plays a significant role in CNT studies and we summarize dispersion techniques to generate airborne CNTs from suspensions or powders. We describe in detail our technique of CNT aerosolization with controlled degree of agglomeration using an electrospray system. The results of animal inhalation studies using the electrosprayed CNTs are presented. We have performed filtration experiments for CNTs through a screen filter. A numerical model has been established to simulate the CNT filtration experiments. Both the modeling and experimental results show that the CNT penetration is less than the penetration for a sphere with the same mobility diameter, which is mainly due to the larger interception length of the CNTs. There is a need for instruments capable of fast and online measurement of gas-borne nanoparticle agglomerates. We developed an instrument Universal NanoParticle Analyzer (UNPA) and the measurement results for diesel exhaust particulates are presented. The results presented here are pertinent to non-spherical aerosol particles, and illustrate the effects of particle morphology on aerosol behaviors.

Keywords

carbon nanotubes; electrospray; toxicity; filtration; nanoparticle agglomerates; diesel exhaust particles

1. Introduction

CNTs are being used in structural composites for sporting equipment, conductive plastics, electron field emitters, semiconductor devices, etc (Wang et al. 2011a). Multi-wall CNTs (MWCNTs) may have diameters about 85 nm and lengths from 2 to 10 μm (Kim et al. 2010), which are similar to the dimensions of asbestos fibers. Such similarity has raised concerns that CNTs may cause negative health effects similar to asbestos fibers. Wick et al. (2007) showed that while suspended CNT-bundles were less cytotoxic than asbestos, rope-like agglomerates induced more pronounced cytotoxic effects than asbestos fibers at the same concentrations. Poland et al. (2008) reported that CNTs introduced into the abdominal

cavity of mice showed asbestos-like pathogenicity in a pilot study. Takagi et al. (2008) and Sakamoto et al. (2009) reported that MWCNTs caused mesothelioma in mice and rats, which is often correlated to asbestos exposure.

Dispersion plays a significant role in CNT studies as CNTs often form large agglomerates of the order of microns when provided by manufacturers in the powder form (Kim et al. 2010). Such large agglomerates have limited mobility, and are easier and safer to handle and transport. Because of their geometry and hydrophobic surface, CNTs have a tendency to form agglomerates with a bundle-like form in aqueous media (Wick et al 2007). Wick et al. studied the effect of degree and kind of agglomeration of CNTs on their cytotoxicity. Davoren et al. (2007) reported the limitation of the instillation method for in vivo or in vitro experiments in several toxicity studies of CNTs, which highlighted the inherent difficulty in testing CNTs due to their agglomerative nature in aqueous media. They suggested further examination using more realistic in vivo inhalation studies with aerosolized CNTs, which were also suggested by Muller et al. (2006). Recently more inhalation studies using airborne CNTs have been reported. Mitchell et al. (2007) studied pulmonary and systemic immune response to inhaled MWCNTs. Shvedova et al. (2008) performed an inhalation study of single-walled CNTs (SWCNTs) on the effect of inflammation, fibrosis, oxidative stress, and mutagenesis. Ryman-Rasmussen et al. (2009a, b) and Pauluhn (2010) studied the effect of inhaled CNTs in the airway system. Kim et al. (2010) used an electrospray system to disperse MWCNTs and exposed rats to the airborne CNTs.

Researchers have developed different methods to disperse CNTs in the aerosol form. Maynard et al. (2004, 2007) used a mechanical agitation method (a vortex shaker) to aerosolize CNT powders. Lee et al. (2009) used a mechanical agitation method (a shaker) and an atomizing method to aerosolize CNT powders and suspensions, respectively. Seto et al. (2010) generated airborne MWCNTs using a Collison atomizer for filtration studies. Mitchell et al. (2007) employed a screw feeder, jet mill, and cutpoint cyclone to produce a respirable aerosol. Baron et al. (2008) used an acoustic feeder system to generate small puffs of CNT powders, which then went through a high-speed knife mill so that the CNT agglomerates may be broken up. The resulting aerosol was size-separated using a settling chamber and two cyclones to produce a respirable aerosol. McKinney et al. (2009) used an acoustic drum to agitate CNTs powders placed on a diaphragm and the resulted airborne CNTs were used for inhalation studies. The above acoustic systems generated CNTs in some degree of agglomeration and the aerodynamic diameter was of the order of several microns. Myojo et al. (2009) used a Palas RBG-1000 aerosol generator to apply mechanical stress to the MWCNTs by a rotating brush, then fed the particles to a two-component fluidized bed to generate aerosols. Ku and Kulkarni (2009) used a capillary electrospray to aerosolize SWCNTs and found that monodisperse SWCNT aerosols below 100 nm were mostly non-agglomerated single fibers, whereas polydisperse aerosols above 100 nm had two distinct morphologies: a ribbon shape and the long, straight fiber. Jennerjohn et al. (2010) used an electrospray system to aerosolize four types of SWCNTs and one type of MWCNTs. We have developed an electrospray system to aerosolize CNTs with controlled degree of agglomeration (Kim et al. 2010, Wang et al. 2011c). The details of this method and animal inhalation results for MWCNTs are described in Section 2. We summarize different CNT aerosolization methods in Table 1.

Filtration is one of the primary technologies for nanoparticle control. Significant research has been performed on filtration of asbestos and fibrous aerosols (Feigley 1975; Gallily et al. 1986; Spurny 1986; Gentry et al. 1989; Gradoń, et al. 1988, 1991; Gradoń and Podgórski 1990; Myojo 1999; Cheng et al. 2006; Webber et al. 2007; Vallero et al. 2009). However, the studies on the filtration of CNTs in air are still scarce (Seto et al. 2010, Wang et al. 2011a, b). Our capability of generating large amount of airborne CNTs facilitates filtration

studies. We have measured penetration of MWCNTs through a metal screen filter. The experimental results and numerical model for CNT filtration are presented in Section 3.

Many nanomaterials are manufactured in the form of nanoparticle agglomerates, which are made up of clusters or chains of nanosize spheres referred to as primary particles. High temperature processes are used to manufacture a variety of materials in agglomerate form including silver, fumed silica, titanium dioxide, and carbon black (Pratsinis 1998, Kim et al. 2009a). Diesel particulate and soot from building fires are also known to be in agglomerated form (Kim et al. 2009b). Agglomerates may possess complicated structures, which makes measurement a difficult task. One of the most common methods for agglomerate measurement is electron microscopy, which can provide direct measurement of the structural properties (Koylu et al. 1995, Rogak et al. 1993, Shin et al. 2009 among many others). However, taking electrical micrographs and performing image analysis can be time consuming and expensive. Fast and online measurement for agglomerates is required in many scenarios including measuring fast changing agglomerates, quality control for material manufacturing, monitoring toxic air-borne agglomerates, etc. Most of the current aerosol instruments are designed for spherical particles. Therefore, there is a need for instruments capable of fast and online measurement of gas-borne nanoparticle agglomerates.

We have developed an instrument, Universal NanoParticle Analyzer (UNPA), for online measurement of gas-borne nanoparticle agglomerates (Wang et al. 2010, Shin et al. 2010). It is based on combined measurement of electrical mobility and unipolar charging properties. The UNPA can provide morphology information of airborne nanoparticles, and determine the primary sphere size if the agglomerates are composed of primary spheres with a fractal dimension less than two (loose agglomerates). We have used the UNPA to measure diesel exhaust particulates and the results are described in Section 4.

2. CNT Dispersion and Animal Inhalation Exposure Test

We developed an electrospray system to disperse and aerosolize CNT colloidal suspensions (Kim et al. 2010, Wang et al. 2011c). The main features of our method are that CNTs with controlled degree of agglomeration can be generated and the output is high compared to other electrospray-based methods. A syringe pump is used to inject the CNT suspensions into a capillary tube. The liquid exiting through the capillary tube is exposed to a strong electric field. The non-uniform electric field causes the liquid meniscus to assume a conical shape established by the balance between the surface tension force and electrical force on the cone. Very small liquid droplets containing CNTs come out of the tip of the capillary. This mechanism can produce droplets in a narrow size distribution, with the peaks ranging from 20 to 500 nm in diameter depending on the liquid conductivity and suspension flowrate. The liquid evaporates quickly and airborne CNTs are obtained. High electrical charges on the electrosprayed nanoparticles lead to repulsion forces, which help to keep the particles separated and free of agglomerates.

Figure 1 illustrates the electrospray system for CNT aerosolization. To achieve high throughput (up to 2 mg/m^3), a large capillary (ID 2.0 mm, OD 3.2 mm), high suspension flow rate (up to 9 ml/hr), and a focusing shield with sheath air are used in the electrospray. The focusing shield (ID 6.35 mm) narrows the spray angle and reduces particle loss on the chamber wall. Four Po-210 sources (185 MBq each) are installed in the neutralization chamber in order to minimize electrostatic particle losses during the particle transportation to the animal inhalation chamber. The locations of radioactive sources in the neutralization chamber were carefully chosen to ensure that the entire charge-reduction zone is covered by α particles emitted from the sources while not allowing ions of opposite polarity of the

applied voltage to travel upward to reach the spray capillary. This minimizes the potential interference of the spray process due to the neutralization of liquid meniscus surface.

MWCNTs (MWCNT-7, OD: 50–85 nm, length: up to ~40 μm, Mitsui Co., Japan) were used in our study. The CNT powder was dispersed in the suspension using a bath type ultrasonicator for more than 24 hrs. Ethanol was used as the carrier liquid to control the conductivity of the nanoparticle suspensions and increase the dispersibility of MWCNT. Figure 2 shows the airborne MWCNT size distribution with peaks around 150 and 400 nm, which represent a single MWCNT peak and a MWCNT bundle peak, respectively. The airborne MWCNT size range was similar to those observed by Lee et al. (2009) and Seto et al. (2010). We can control the degree of agglomeration by changing the MWCNT suspension flowrate, because a higher flow rate generates bigger droplet sizes with more MWCNTs in each droplet. Figure 3a shows airborne MWCNTs sampled by an electrostatic precipitator with a suspension flow rate of 3 ml/hr, demonstrating that the particles are well-dispersed and that some maintain a rigid, needle-like shape. Figure 3b shows electrosprayed MWCNTs at a higher flow rate (9 ml/hr), which shows a higher degree of agglomeration. The ability to change the agglomeration degree gives us flexibility in simulating CNTs in realistic emissions.

Animal inhalation tests were performed using the CNT aerosols. We generated airborne MWCNTs with a suspension flow rate of 3 ml/hr, and the rats were exposed to the CNTs in the inhalation chamber for 4 hrs at a concentration of 800 $\mu g/m^3$. At 20 hrs post-exposure, animals were killed by an overdose of i.p. pentobarbital, the lungs were excised and lavaged 5 times with saline. After centrifugation (400 g, 10 mins) the lavaged cells were examined by light and scanning electron microscopy. The images (Fig. 4) showed that alveolar macrophages contained the electrosprayed MWCNTs; the shorter ones agglomerated inside macrophages and the longer ones were only partly phagocytized, which might cause irritation to the lung.

3. Experimental and Modeling Studies of CNT Filtration

We have performed filtration experiments using the electrosprayed airborne CNTs (Wang et al. 2011a, b). The CNTs were classified by a different mobility analyzer (DMA), then passed through a Po-210 neutralizer and the selected CNTs with the same electrical mobility size were used to challenge the filter. The concentrations upstream and downstream of the filter were measured by a condensation particle counter (CPC). Then the fractional penetration through the filter was obtained. The testing filters were screens made of 635-mesh type 304 stainless steel, which are used in the diffusion battery (TSI, model 3040). The screen wire is 20 μm in diameter and the opening dimension is also 20 μm (Fig. 5). Figure 6 shows the measured penetration values of CNTs and polystyrene latex (PSL) spheres as functions of the mobility size. PSL particles were used to provide the control data set. When the mobility size is above 100 nm, the penetration of CNTs is considerably lower than that of PSL spheres. The interception mechanism plays an important role in this size range. The CNTs have open structures and larger interception lengths than spheres, thus lower penetration.

We developed a numerical model for fibrous filtration using the computational fluid dynamics code FLUENT (Wang et al. 2008a, b, Wang and Pui 2009). Simulations for CNTs pose new challenges since their motion in air flow is more complicated than spherical particles. A three-dimension model including two perpendicular cylinders with 20 μm diameter and 40 μm height is created to simulate the cross-shaped section (Fig. 7) of the screen filter. The simulation domain is a long box with a 40 μm by 40 μm cross-section and the two cylinders are placed at the center of the domain. The inlet of the flow is 200 μm

upstream to the first cylinder and a uniform velocity profile is prescribed. The outlet of the flow is 200 μm downstream to the second cylinder and the derivatives normal to the outlet plane are set to be zero. No-slip condition is used on the cylinder surfaces. Symmetric conditions are used on the four sides of the simulation domain. Mesh with tetrahedral cells is used to discreticize the simulation domain.

The flow field is obtained by solving the steady-state incompressible Navier-Stokes equations. Mechanisms for particle capture include diffusion, interception, inertial impaction, electrostatic effect and gravitational settling. Here we consider neutral particles thus the electrostatic effect is not involved. Gravitational settling is usually negligible for nanoparticles. Numerical study of the particle capture due to diffusion may be carried out by solving the convective diffusion equation

$$\mu_i \frac{\partial}{\partial x_i} n = D \frac{\partial^2}{\partial x_i^2} n, \quad (1)$$

where u_i is the ith component of the flow velocity, D is the diffusion coefficient and n is the particle concentration. The particle concentration is obtained by solving (1), then penetration when diffusion is the only capture mechanism, is computed as

$$P_n^D = n_{outlet} / n_{inlet}, \quad (2)$$

where n_{outlet} and n_{inlet} are the average particle concentrations at the outlet and inlet, respectively. To simulate particle capture due to interception and inertial impaction, we add particles to the flow using the Discrete Phase Model. This model calculates the trajectories of particles using a Lagrangian formulation that includes the particle inertia and hydrodynamic drag. The governing equation of the particle motion is

$$m \frac{dv}{dt} = F_d, \quad (3)$$

where m is the particle mass, v is the particle velocity, t is the time and F_d is the drag on the particle. Equation (3) gives the trajectory of the center of particle mass. Rotation and thus spatial orientation of non-spherical particles can be obtained by solving the torque equation. We do not solve the torque equation for each individual particle, instead, the effects of particle orientation on the drag, diffusion coefficient and interception length are considered in the sense of average over a large number of fibrous particles. The particle size and interception are taken into account by a User Defined Function (Wang and Pui 2009). We assume a particle is permanently captured when it comes into contact with a filter fiber, which is widely accepted in classical filtration theory because of the strong van der Waals force between nanoparticles and filter fibers. We release a large number of particles distributed evenly in the cross-section upstream to the filter and track their movement. The number of particles that escape at the outlet is determined and we can compute the penetration. The particle deposition is due to the combined effects of inertial impaction and interception, and the penetration will be denoted as P_n^{I+R}. The total penetration when mechanical mechanisms for particle capture are considered is then

$$P_n = P_n^D \cdot P_n^{I+R}. \quad (4)$$

We discuss application of the general numerical model to filtration of CNTs by the screen filter. The length, diameter and mass of CNTs need to be determined for the simulation. We utilized the DMA to select CNTs of a certain mobility diameter and analyzed them by SEM.

This allowed us to determine the CNT length as a function of the mobility diameter. Our results show that the mean CNT length was 2300 nm, 4300 nm and 6100 nm when the CNT mobility diameter was 200 nm, 300 nm and 400 nm, respectively. The geometric diameter of the CNTs was d_{CNT} = 85 nm for the MWCNTs in our experiments. Kim S.H. et al. (2009) reported that the density of size-selected MWCNTs was 1.74 g/cm^3 measured by a mobility-mass method. With the length, diameter and density, we can compute the mass of CNTs for different values of their mobility diameter.

Next consider the drag force and diffusion coefficient of CNTs, which can be computed based on their mobility diameters. However, the orientation of the CNTs may be different in the DMA and the filter. Short CNTs may rotate freely in the DMA, but long CNTs may be aligned with the electrical field. Kim S.H. et al. (2007) showed that CNTs with the aspect ratio larger than 30 would align with the electrical field in the DMA. Following their results, we find that for short CNTs (with the mobility diameter dm less than 213 nm), the orientation is random in both the DMA and the filter, thus the drag and diffusion coefficient of short CNTs in the filter are the same as those of spheres with the same mobility diameter. For long CNTs (with the mobility diameter dm larger than 213 nm), the orientations in the DMA and in the filter are different, thus the drag force on the long CNTs in the filter is larger than that in the DMA, and the diffusion coefficient in the filter is smaller than that in the DMA.

Interception is considered to occur if any point on a CNT contacts a wire in the screen filter. The interception length is determined based on the CNT length and the average angle between the CNT and the filter wire surface. We found that the CNT interception length was much larger than their mobility diameters, which is the main explanation for that the CNT penetration is less than that for a sphere with the same mobility diameter, as observed in the experiments.

The simulation results for CNT penetration are compared to the experimental ones as shown in Fig. 8. Simulation is also carried out for spherical PSL particles and the agreement between the model and experiments is excellent. This demonstrates that our general numerical methods are sound. For the CNTs, the modeling results agree reasonably well with experiments when d_m < 250 nm, but significantly underestimate the penetration when d_m > 250 nm. Both the modeling and experimental results show that the CNT penetration is less than the penetration for a sphere with the same mobility diameter, which is mainly due to the larger interception length of the CNTs. One reason for underestimation of the penetration of longer CNTs (d_m > 250 nm) may be that they curl or bend in the flow, which makes their effective interception length smaller and easier to penetrate the filter. Examples of SEM images of electrosprayed CNTs in Figures 2, 3, and 6 show that both straight and curled CNTs exist. Gradoń and Podgórski (1990) showed that perfectly flexible elongated particles can deform and align with the streamline and pass by the filter element. Our CNTs are not perfectly flexible but the longer CNTs may bend in the flow and the results agree qualitatively with Gradoń and Podgórski (1990). We used CNT suspensions with low concentrations in the filtration study, thus the agglomeration degree was low and we obtained many single CNTs as shown in SEM images (Wang et al. 2011b). Nevertheless, it is possible that agglomeration has some impact on the filtration results when the mobility diameter is over 250 nm, since the agglomeration degree increases with the mobility diameter. The CNT agglomerates are more compact than individual CNTs, therefore their interception length is smaller than that of the individual CNTs of the same mobility diameter, which leads to higher penetration for the CNT agglomerates.

4. Measurement of Agglomerates using the Universal NanoParticle Analyzer (UNPA)

We have developed the instrument UNPA, for online measurement of gas-borne nanoparticle agglomerates (Wang et al. 2010, Shin et al. 2010). UNPA utilizes DMA, CPC and Nanoparticle Surface Area Monitor (NSAM) to characterize airborne nanoparticle morphology and measure the number, surface area and volume distributions of airborne nanoparticles. The key parameter measured is the UNPA sensitivity, which is defined as the current I(fA) measured by the NSAM divided by the number concentration N(#/cm^3) measured by the CPC

$$S = I/N(\text{fA cm}^3). \quad (5)$$

Charging theories of Chang (1981) for aerosol particles of arbitrary shape indicate that the geometric surface area and electrical capacitance of the particles are two important parameters to determine the mean charge of non-spherical particles. The electrical capacitance of agglomerates may be computed using a variational method proposed by Brown and Hemingway (1995). The surface area of loose agglomerates may be calculated using a mobility analysis developed by Lall and Friedlander (2006). Shin et al. (2010) combined the above analyses to show that the electrical capacitance of loose agglomerates is larger than that of spherical particles with the same mobility, and loose agglomerates can gain more charges from unipolar charging.

The primary particle size plays an important role in determination of the surface area and electrical capacitance, thus the charges on agglomerates. The UNPA sensitivity is related to the primary particle diameter d_p. We found that the UNPA sensitivity can be correlated to the primary particle size through a power law relation (Wang et al. 2010)

$$S = c_2\left(\frac{12\pi\lambda}{c^* d_p^2}\frac{d_m}{C_c}\right)^k c_1 (d_p)^h \quad (6)$$

where c^* is a constant regarding particle orientation, λ is the mean gas free path, c_1, c_2, k and h are constants which can be determined from the experimental data. Then the sensitivity data from the experiments can be fitted into (6) to determine the primary particle diameter d_p. Once the primary particle size is determined, surface area and volume of the agglomerates can be calculated.

Diesel engine exhaust has profound impact on environment and ecosystem. Diesel aerosols are mainly agglomerates with open structures and composed of primary particles (Fig. 9). We measured diesel aerosols generated from a 4045 John Deere Diesel Engine using UNPA. A schematic of the experiment is shown in Fig. 10. Diesel aerosols were sampled form the exhaust pipe and mixed with dilution air in the residence chamber. Then the diesel aerosols were sent to Nanometer Aerosol Sampler (NAS) for collection of electron micrograph samples, and to UNPA for agglomerate measurement.

We sampled the diesel aerosols under two engine conditions: light load and heavy load. The engine speed, torque and exhaust temperature increased with the load. A catalytic stripper was used to remove sulfur compounds and the soluble organic fraction by passing the diluted diesel exhaust over two heated catalysts. The primary particle sizes of diesel particles measured by UNPA are listed in Table 2. The UNPA sensitivities and the primary particle sizes for the diesel particles with and without the catalytic stripper are nearly identical. The result indicates that the coating of the soluble organic fraction does not change

the particle morphology significantly, neither does it change the charging properties of the particles substantially, since the material effect is only a secondary effect on diffusion charging. The result is consistent with past results showing that the adsorbed materials on diesel soot particles have little influence on the mobility size (Kittelson et al. 2005). The primary sizes were also measured using a large number of TEM images. A total of 212 primary particles were analyzed in the case of heavy load, and 189 primary particles in the case of light load. The primary particle size from TEM agreed well with UNPA measurement for the heavy load case. In the case of light load, there was about 6 nm difference between UNPA and TEM results, which was still within the standard deviation of the TEM result.

5. Summary

We discuss dispersion and filtration of CNTs and measurement of nanoparticle agglomerates in diesel exhaust. A number of techniques to generate airborne CNTs from powders or suspensions are reviewed, including mechanical shakers, mills, fluidized beds, acoustic drums, atomizers and electrosprays. We have developed an electrospray system to aerosolize CNTs from suspensions, and the agglomeration degree increases with the flow rate of the suspension. We used electrosprayed MWCNTs for animal inhalations studies and found the CNTs in alveolar macrophages. We also used the electrosprayed MWCNTs for a filtration study. The penetration of CNTs through a metal screen was shown to be significantly lower than spheres of the same mobility size. A numerical model was established to simulate the CNT filtration experiments. The results indicate that the larger interception lengths of the CNTs were the main reason for the lower penetration.

Nanoparticle agglomerates possess different electrical charging properties than spherical particles, which is the basis of our instrument Universal NanoParticle Analyzer (UNPA). UNPA measurement results for diesel exhaust particulates agreed well with offline measurements.

Highlights

- A summary of the dispersion techniques for airborne carbon nanotubes (CNTs) is presented.
- CNT aerosolization by electrospray and the toxicity study with the CNTs are presented.
- Filtration of airborne CNTs is investigated both experimentally and numerically.
- Diesel exhaust particulates are measured with the Universal NanoParticle Analyzer.

Acknowledgments

The work was partially supported by the US National Institute of Environmental Health Sciences grant “Hazard Assessment and Risk Estimation of Inhaled Nanomaterials Exposure” # 1RC2ES018741-01 (sub-grant 100029-D) and by the Swiss National Science Foundation grant “Evaluation platform for safety and environmental risks of carbon nanotube reinforced nanocomposites” 406440_131286.

References

Baron PA, Deye GJ, Chen BT, Schwegler-Berry DE, Shvedova AA, Castranova V. Aerosolization of Single-Walled Carbon Nanotubes for an Inhalation Study. Inhalation Toxicology. 2008; 20:751–760. [PubMed: 18569097]

Brown RC, Hemingway MA. Electric charge distribution and capacitance of agglomerates of spherical particles: theory and experimental simulation. J. Aerosol Science. 1995; 26:1197–1206.

Chang J-S. Theory of diffusion charging of arbitrarily shaped conductive aerosol particles by unipolar ions. J. Aerosol Science. 1981; 12:19–26.

Cheng YS, Holmes TD, Fan B. Evaluation of respirator filters for asbestos fibers. J Occup Environ Hyg. 2006; 3(1):26–35. [PubMed: 16482975]

Davoren M, Herzog E, Casey A, Cottineau B, Chambers G, Byrne HJ, Lyng FM. In vitro toxicity evaluation of single walled carbon nanotubes on human A549 lung cells. Toxicol In Vitro. 2007; 21:438–448. [PubMed: 17125965]

Feigley CE. A mathematical model for deposition of asbestos in fibrous filter. Clean Air (Heidelberg, Aust.). 1975:67–71.

Gallily I, Schiby D, Cohen AH, Hollander W, Schless D. On the Inertial Separation of Nonspherical Aerosol Particles from Laminar Flows. I. The Cylindrical Case. Aerosol Sci. Tech. 1986; 5:267–286.

Gentry GW, Spurny K, Schörmann D. Collection efficiency of ultrafine asbestos fibers, experimental and theory. Aerosol Sci. Technol. 1989; 9:184.

Gradoñ L, Podgórski A. Flexible fibrous particle behaviour in the carrier gas flow around cylindrical obstacle. Chem. Engng Sci. 1990; 45:3435.

Gradoñ L, Podgórski A, Grzybowski P. Deposition of flexible and stiff fibrous particles. Journal of Aerosol Science. 1991; 20:971–974. 1989.

Gradoñ L, Grzybowski P, Piłaciński W. Analysis of motion and deposition of fibrous particles on a single filter element. Chem. Engng Sci. 1988; 43:1253–1259.

Jennerjohn N, Eiguren-Fernandez A, Prikhodko S, Fung DC, Hirakawa KS, Zavala-Mendez JD, Hinds W, Kennedy NJ. Design, demonstration and performance of a versatile electrospray aerosol generator for nanomaterial research and applications. Nanotechnology. 2010; 21:255603. [PubMed: 20516581]

Kim SC, Chen DR, Qi C, Gelein RM, Finkelstein JN, Elder A, Bentley K, Oberdorster G, Pui DYH. A nanoparticle dispersion method for in vitro and in vivo nanotoxicity study. Nanotoxicology. 2010; 4(1):42–51. [PubMed: 20795901]

Kim SC, Wang J, Emery M, Shin W-G, Mullholand G, Pui DYH. Structural Property Effect of Nanoparticle Agglomerates on Particle Penetration through Fibrous Filter. Aerosol Sci. & Technology. 2009a; 43(4):344–355.

Kim SC, Wang J, Shin W-G, Scheckman J, Pui DYH. Structural properties and filter loading characteristics of soot agglomerates. Aerosol Sci. & Technology. 2009b; 43:1033–1041.

Kim SH, Mulholland GW, Zachariah MR. Understanding ion-mobility and transport properties of aerosol nanowires. J. Aerosol Sci. 2007; 38:823–842.

Kim SH, Mulholland GW, Zachariah MR. Density measurement of size selected multiwalled carbon nanotubes by mobility-mass characterization. Carbon. 2009; 47(5):1297–1302.

Kittelson DB, Watts WF, Savstrom JC, Johnson JP. Influence of a catalytic stripper on the response of real time aerosol instruments to diesel exhaust aerosol. J. Aerosol Science. 2005; 36:1089–1107.

Koylu UO, Faeth GM, Farias TL, Carvalho MG. Fractal and projected structure properties of soot aggregates. Combustion Flame. 1995; 100:621–633.

Ku BK, Kulkarni P. Morphology of single-wall carbon nanotube aggregates generated by electrospray of aqueous suspensions. J. Nanoparticle Research. 2009; 11:1393–1403.

Lall AA, Friedlander SK. On-line measurement of ultrafine aggregate surface area and volume distributions by electrical mobility analysis: I. Theoretical analysis. J. Aerosol Science. 2006; 37:260–271.

Lee S-B, Lee J-H, Bae G-N. Size response of an SMPS–APS system to commercial multi-walled carbon nanotubes. J. Nanoparticle Research. 2009; 12:501–512.

Maynard AD, Baron PA, Foley M, Shvedova AA, Kisin ER, Castranova V. Exposure to carbon nanotube material: aerosol release during the handling of unrefined single walled carbon nanotube material. J. Toxicol Environ Health A. 2004; 67:87–107. [PubMed: 14668113]

Maynard AD, Ku BK, Emery M, Stolzenburg M, McMurry PH. Measuring particle size-dependent physiochemical structure in airborne single walled carbon nanotube agglomerates. J. Nanoparticle Research. 2007; 9:85–92.

McKinney W, Chen BT, Frazer D. Computer controlled multi-walled carbon nanotube inhalation exposure system. Inhalation Toxicology. 2009; 21:1053–1061. [PubMed: 19555230]

Mitchell L, Gao J, Vander Wal R, Gigliotti A, Burchiel S, McDonald J. Pulmonary and systemic immune response to inhaled multiwalled carbon nanotubes. Toxicol. Sci. 2007; 100:203–214. [PubMed: 17660506]

Muller J, Huaux F, Lison D. Respiratory toxicity of carbon nanotubes: how worried should we be? Carbon. 2006; 44:1048–1056.

Myojo T. A Simple Method to Determine the Length Distribution of Fibrous Aerosols. Aerosol Sci. & Technology. 1999; 30:30–39.

Myojo T, Oyabu T, Nishi K, Kadoya C, Tanaka I, Ono-Ogasawara M, Sakae H, Shirai T. Aerosol Generation and Measurement of Multi-Wall Carbon Nanotubes. J. Nanoparticle Res. 2009; 11:91–99.

Pauluhn J. Subchronic 13-Week Inhalation Exposure of Rats to Multiwalled Carbon Nanotubes: Toxic Effects Are Determined by Density of Agglomerate Structures, Not Fibrillar Structures. Toxicological Sciences. 2010; 113(1):226–242. [PubMed: 19822600]

Poland CA, Duffin R, Kinloch I, Maynard A, Wallace WAH, Seaton A, Stone V, Brown W, MacNee W, Donaldson K. Carbon nanotubes introduced into the abdominal cavity of mice show asbestos-like pathogenicity in a pilot study. Nature Nanotechnology. 2008; 3:423–428.

Pratsinis SE. Flame aerosol synthesis of ceramic powders. Progress in Energy and Combustion Science. 1998; 24:197–219.

Rogak SN, Flagan RC, Nguyen HV. The mobility and structure of aerosol agglomerates. Aerosol Sci Technol. 1993; 18:25–47.

Ryman-Rasmussen JP, Cesta MF, Brody AR, Shipley-Phillips JK, Everitt JI, Tewksbury EW, et al. Inhaled carbon nanotubes reach the subpleural tissue in mice. Nat Nanotechnol. 2009a; 4(11):708–710. [PubMed: 19893519]

Ryman-Rasmussen JP, et al. Inhaled multiwalled carbon nanotubes potentiate airway fibrosis in a murine model of allergic asthma. Am. J. Resp. Cell. Mol. Biol. 2009b; 40:349–358.

Sakamoto, et al. Induction of mesothelioma by a single intrascrotal administration of multi-wall carbon nanotube in intact male Fischer 344 rats. J. Tox. Sci. 2009; 35:65–76.

Seto T, Furukawa T, Otani Y, Uchida K, Endo S. Filtration of Multi-Walled Carbon Nanotube Aerosol by Fibrous Filters. Aerosol Science and Technology. 2010; 44:734–740.

Shin WG, Wang J, Mertler M, Sachweh B, Fissan H, Pui DYH. Structural properties of silver nanoparticle agglomerates based on transmission electron microscopy: relationship to particle mobility analysis. J. Nanoparticle Research. 2009; 11:163–173.

Shin WG, Wang J, Mertler M, Sachweh B, Fissan H, Pui DYH. The Effect of Particle Morphology on Unipolar Diffusion Charging of Nanoparticle Agglomerates in the Transition Regime. J. Aerosol Science. 2010; 41:975–986.

Shvedova AA, Kisin E, Murray AR, Johnson VJ, Gorerlik O, Arepalli S, Hubbs F, Mercer RR, Keohavong P, Sussman N, Jin J, Yin J, Stone S, Chen BT, Deye G, Maynard AD, Castranova V, Baron PA, Kagan VE. Inhalation versus aspiration of single-walled carbon nanotubes in C57BL/6 mice: inflammation, fibrosis, oxidative stress, and mutagenesis. Am. J. Physiol Lung Cell Mol Physiol. 2008; 295(4):L552–L565. [PubMed: 18658273]

Spurny KR. On the filtration of fibrous aerosols. Science of the Total Environment. 1986; 52:189–199.

Takagi A, et al. Induction of mesothelioma in p53þ/- mouse by intraperitoneal application of multi-wall carbon nanotube. J. Toxicol. Sci. 2008; 33:105–116. [PubMed: 18303189]

Vallero DA, Kominsky JR, Beard ME, Crankshaw OS. Efficiency of sampling and analysis of asbestos fibers on filter media: implications for exposure assessment. J Occup Environ Hyg. 2009; 6(1):62–72. [PubMed: 19037817]

Wang J, Pui DYH. Numerical Investigation of Filtration by Fibers with Elliptical Cross-sections. J. Nanoparticle Research. 2009; 11(1):185–196.

Wang J, Kim SC, Pui DYH. Investigation of the Figure of Merit for Filters with a Single Nanofiber Layer on a Substrate. J. Aerosol Science. 2008a; 39:323–334.

Wang J, Kim SC, Pui DYH. Figure of merit of composite filters with micrometer and nanometer fibers. Aerosol Science & Technology. 2008b; 42:722–728.

Wang J, Kim SC, Pui DYH. Carbon Nanotube Penetration through a Screen Filter: Numerical Modeling and Comparison with Experiments. Aerosol Sci. & Technology. 2011a; 45(3):443–452.

Wang J, Kim SC, Pui DYH. Measurement of Multi-wall Carbon Nanotube penetration through a screen filter and single-fiber analysis. J. Nanoparticle Research. 2011b; 13:5415–5424.

Wang J, Asbach C, Fissan H, Hülser T, Kuhlbusch TAJ, Thompson D, Pui DYH. How can nanobiotechnology oversight advance science and industry: Examples from Environmental, Health and Safety Studies of Nanoparticles (nano-EHS). J. Nanoparticle Research. 2011c; 13:1373–1387.

Wang J, Shin W-G, Mertler M, Sachweh B, Fissan H, Pui DYH. Measurement of Nanoparticle Agglomerates by Combined Measurement of Electrical Mobility and Unipolar Charging Properties. Aerosol Sci. & Technology. 2010; 44:97–108.

Webber JS, Czuhanich AG, Carhart LJ. Performance of membrane filters used for TEM analysis of asbestos. J Occup Environ Hyg. 2007; 4(10):780–789. [PubMed: 17763069]

Wick P, Manser P, Limbach LK, Dettlaff-Weglikowska U, Krumeich F, Roth S, Stark WJ, Bruinink A. The degree and kind of agglomeration affect carbon nanotube cytotoxicity. Toxicology Letters. 2007; 168:121–131. [PubMed: 17169512]

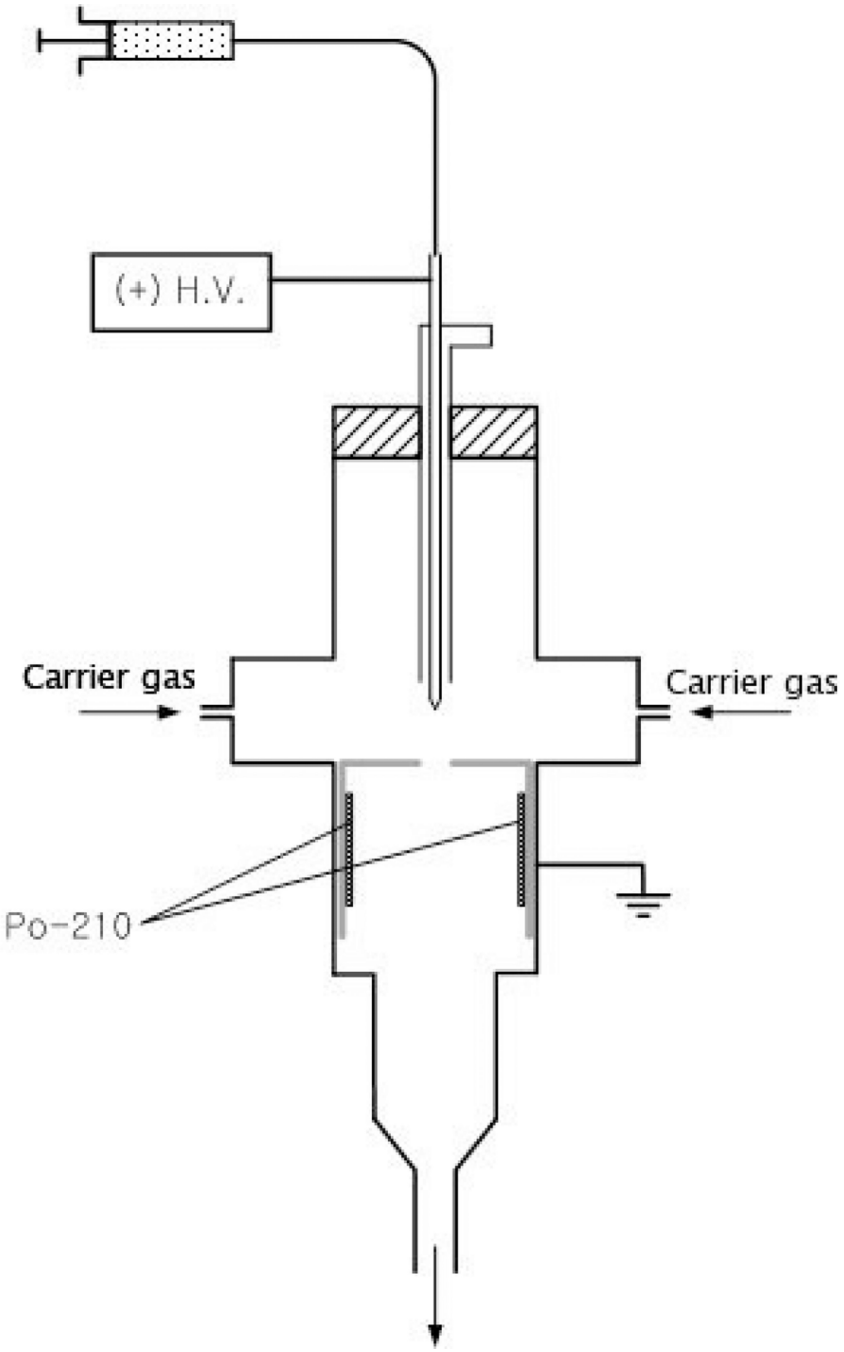

Figure 1.
Schematic of the electrospray system for CNT aerosolization.

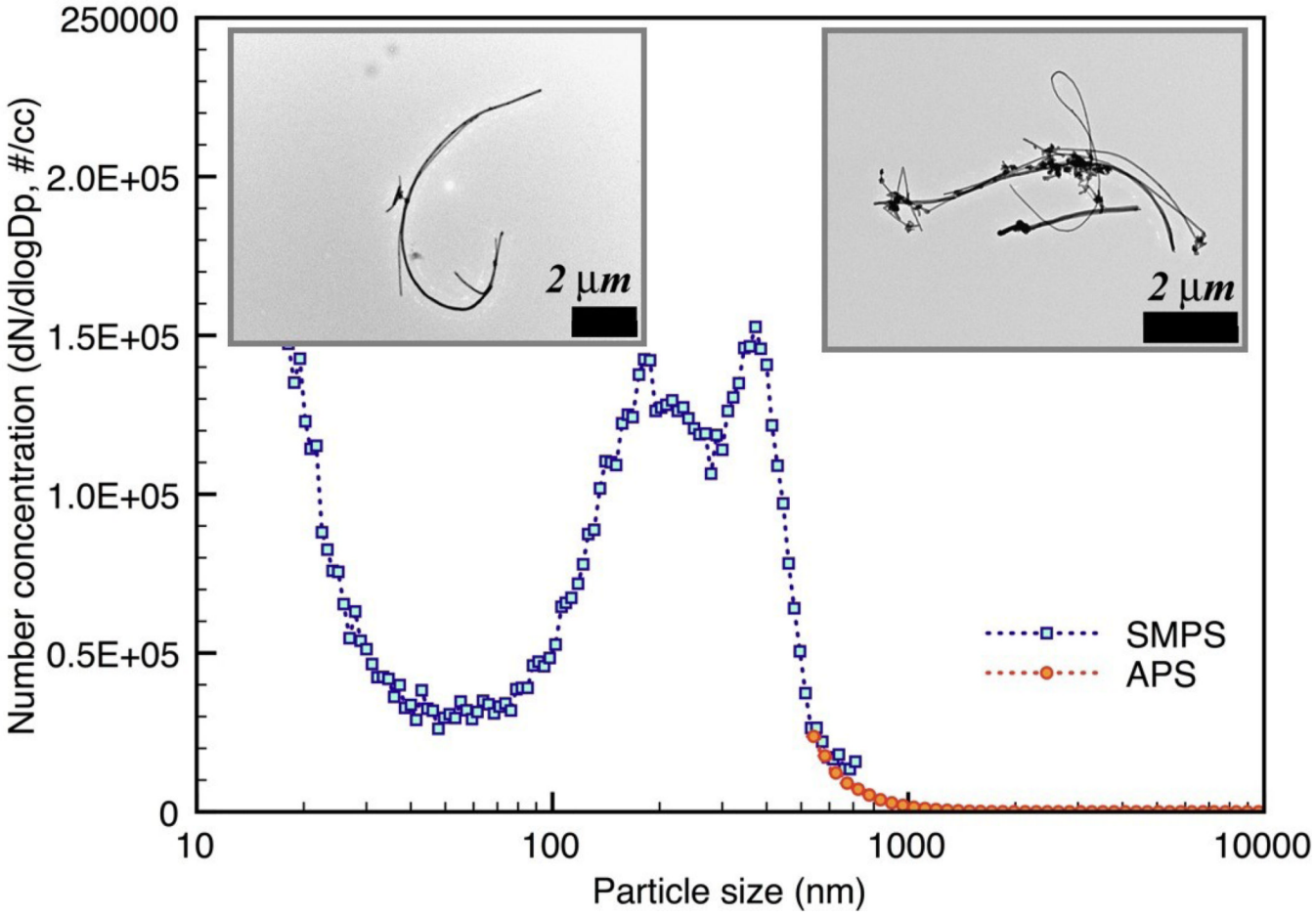

Figure 2.
Number-size distribution of airborne MWCNTs measured by a scanning mobility particle sizer (SMPS) and an aerodynamic particle sizer (APS).

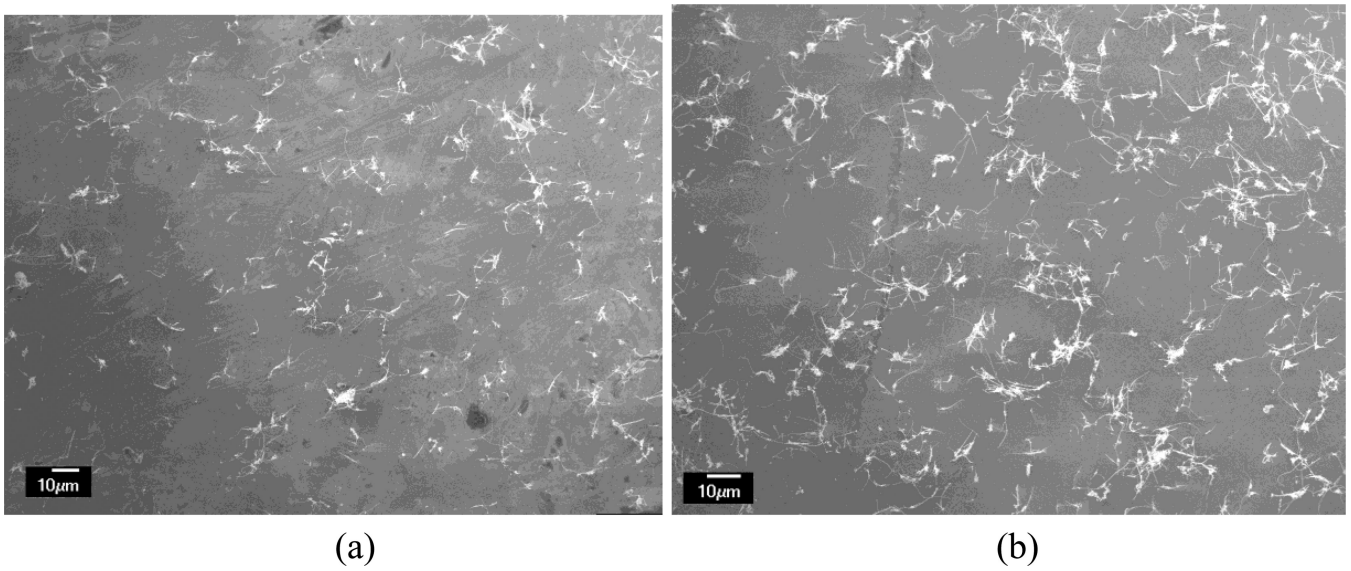

Figure 3.
SEM images of electrosprayed MWCNTs (a) with a suspension flow rate of 3 ml/hr; (b) with a suspension flow rate of 9 ml/hr.

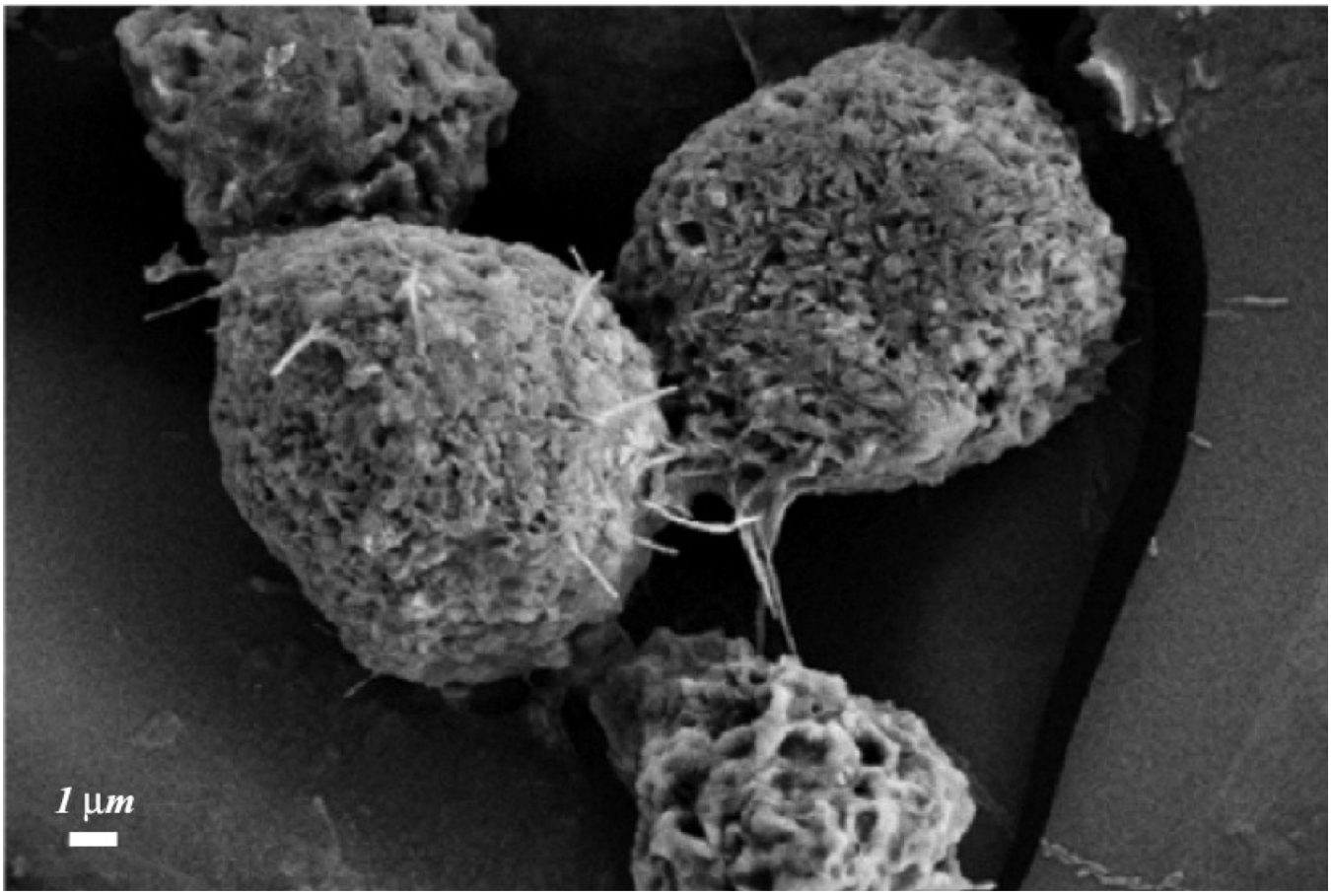

Figure 4.
SEM image of rat alveolar macrophages in lung lavage fluid 20 hrs after electrospray inhalation exposure to MWCNTs.

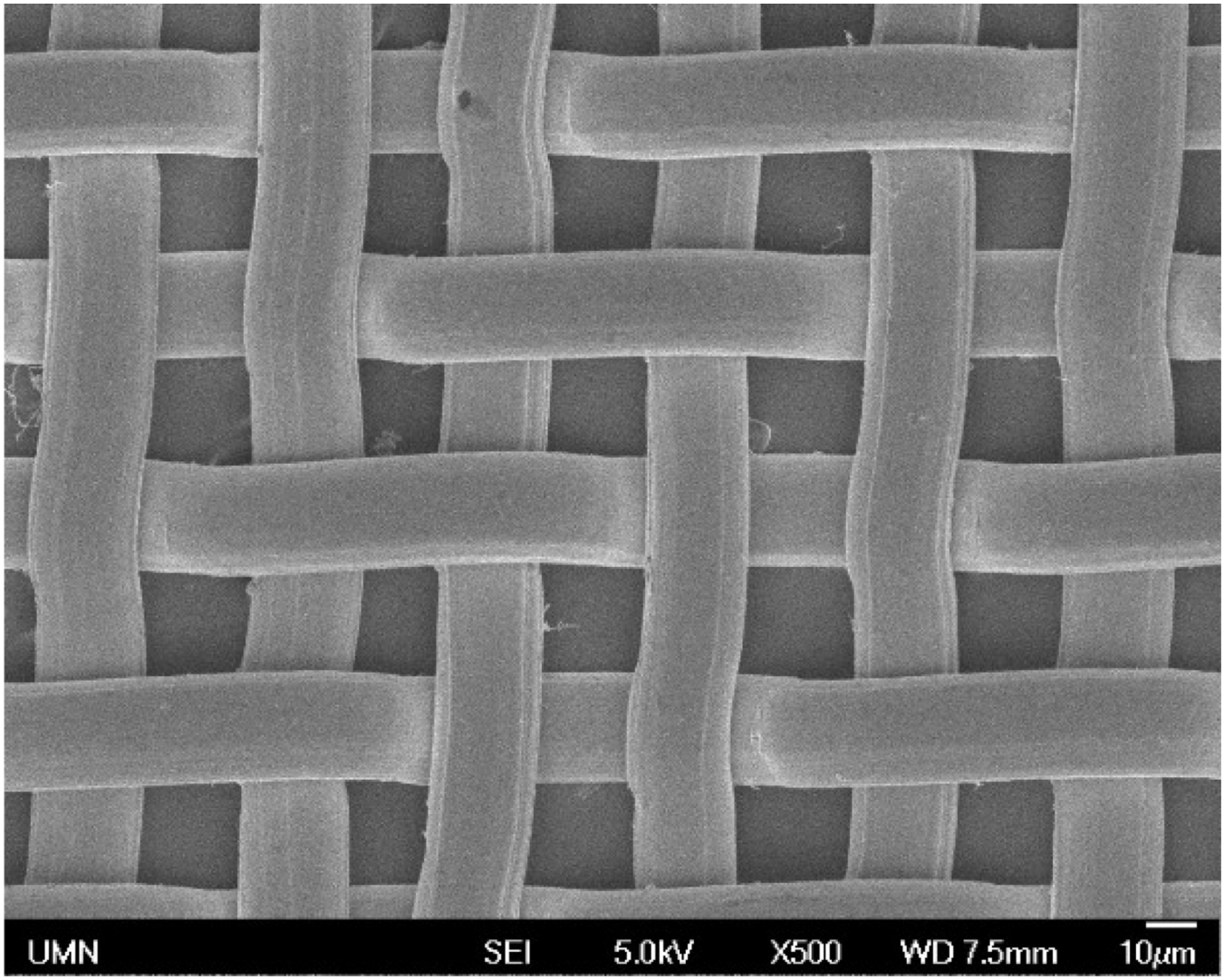

Figure 5.
SEM images of the stainless steel screen used in the filtration tests.

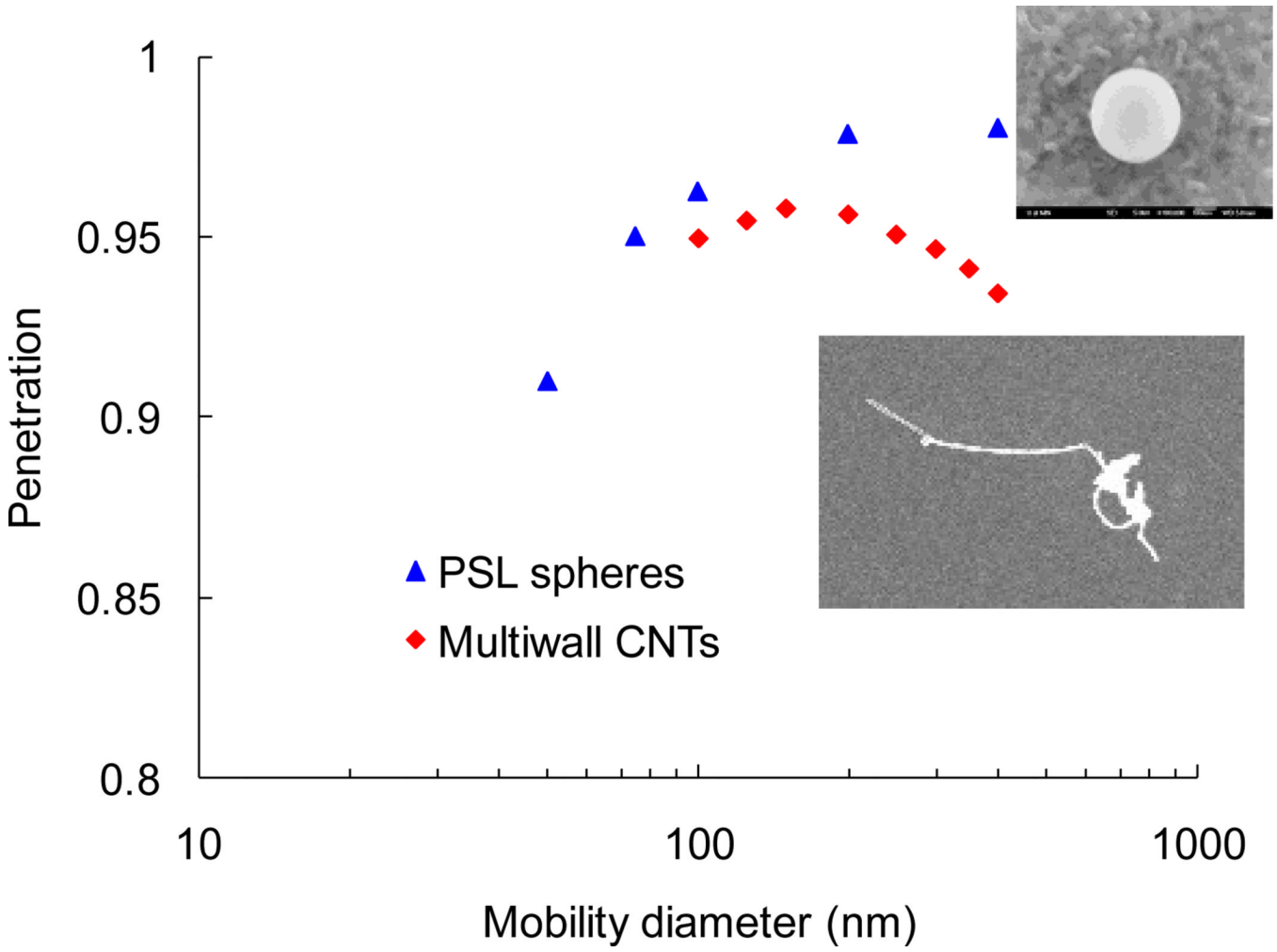

Figure 6.
The measured penetration values of multi-wall CNTs and PSL spheres.

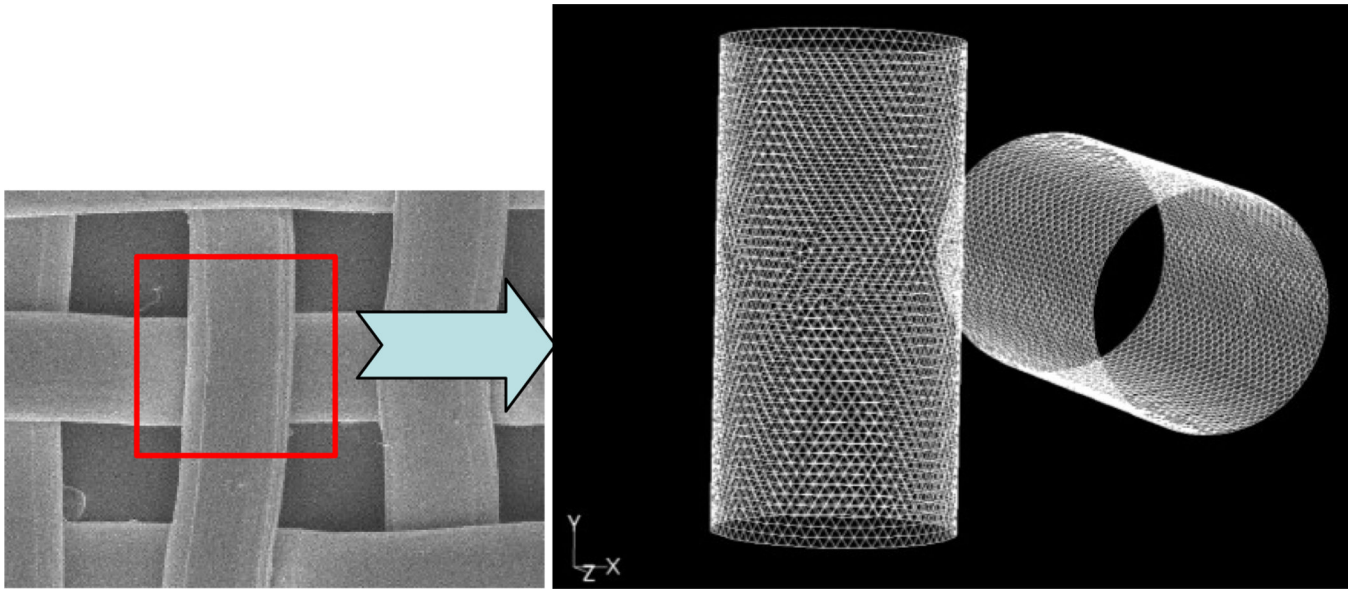

Figure 7.
The three-dimension model for simulation of the cross-shaped section in the screen filter.

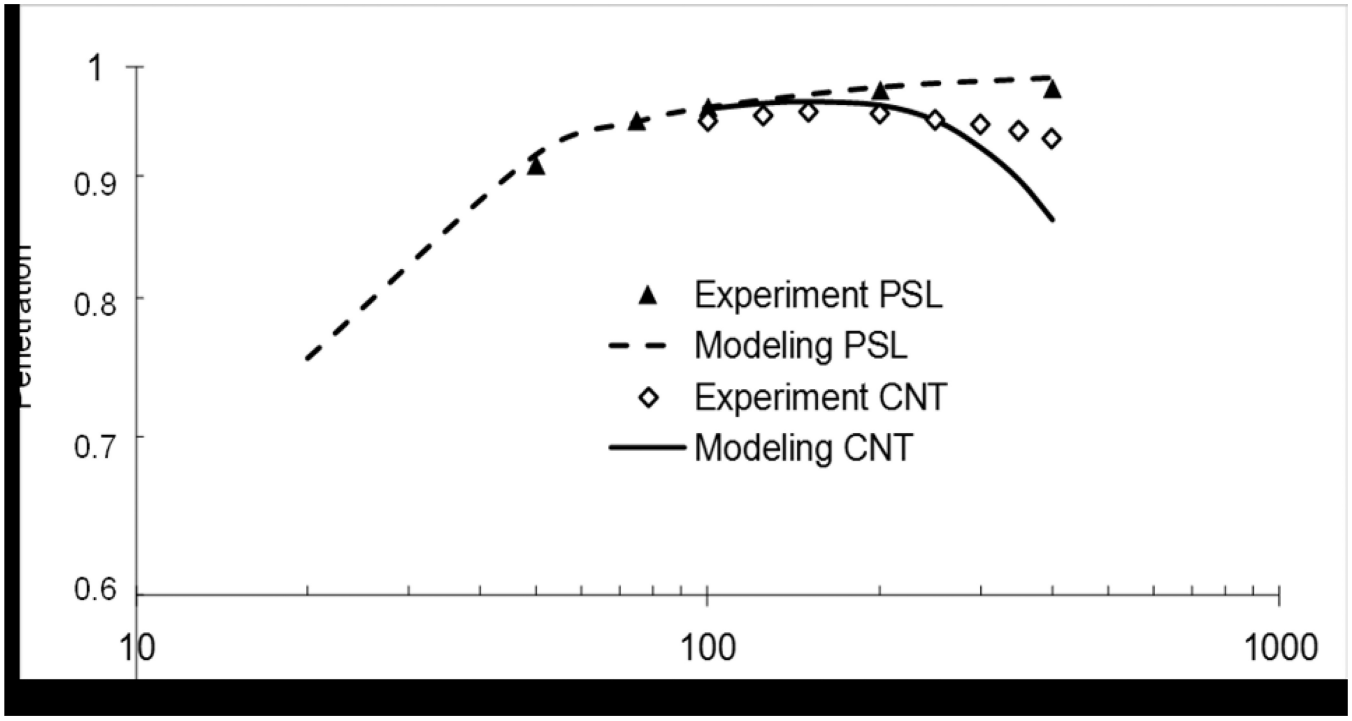

Figure 8.
Penetrations of PSL particles and CNTs through the screen filter as functions of the mobility size d_m.

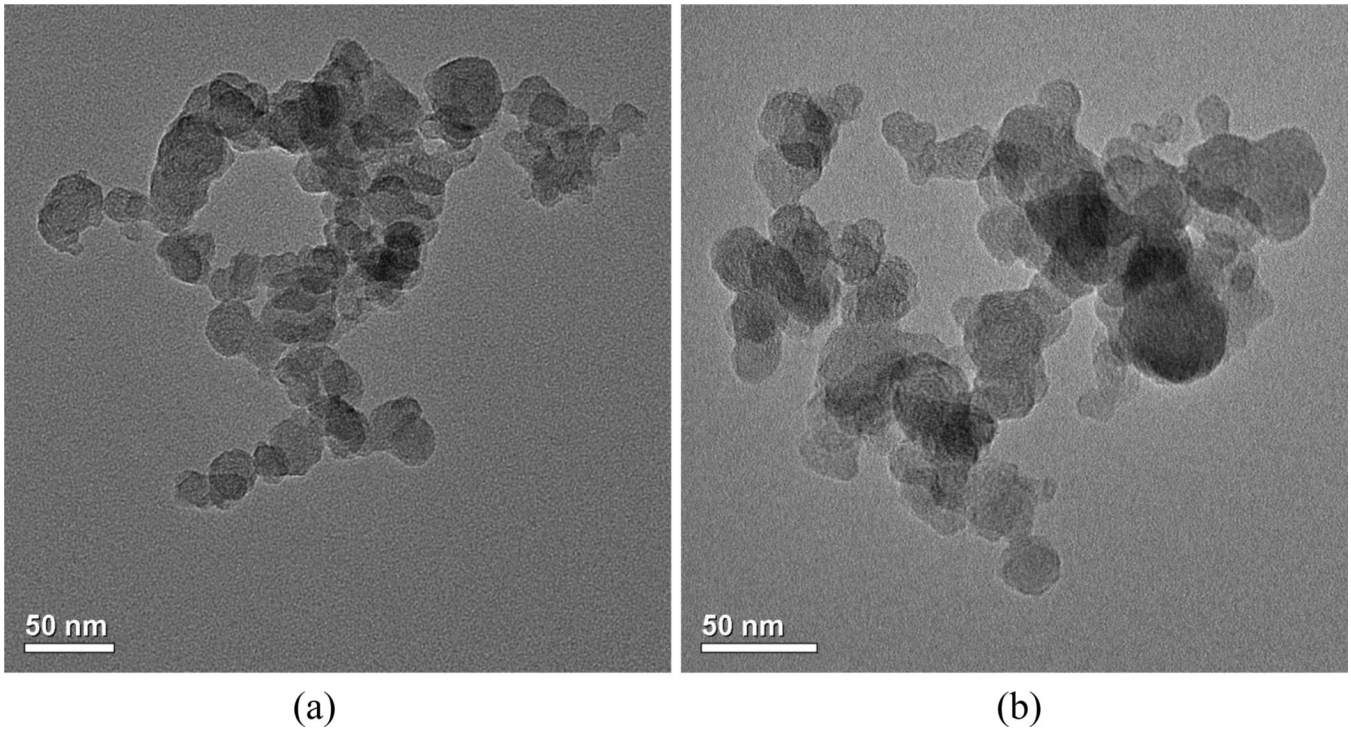

Figure 9.
TEM images of diesel particles under the following conditions (a) light load, (b) heavy load.

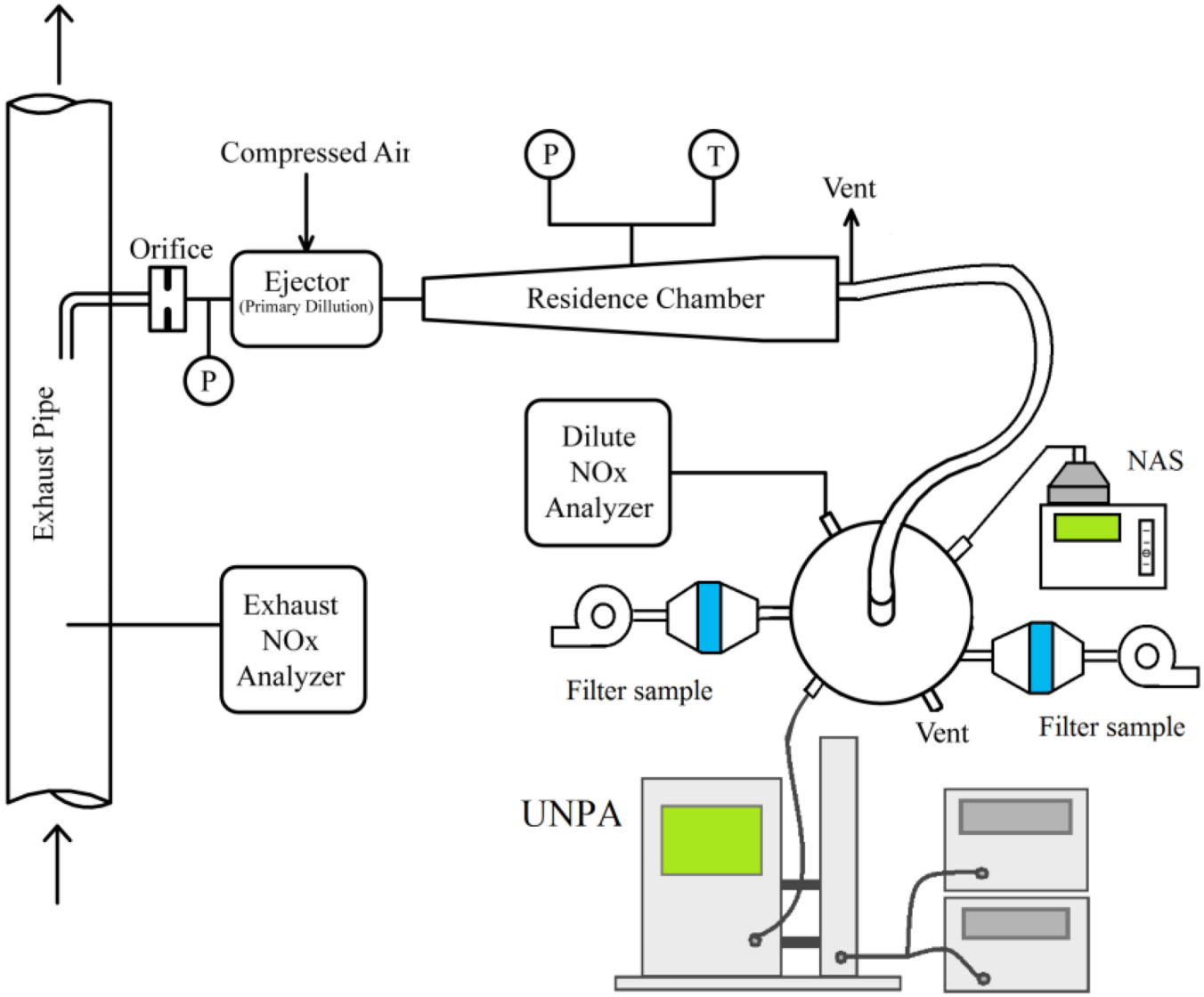

Figure 10.
A schematic of the setup for diesel aerosol sampling and measurement.

Table 1

Summary for CNT aerosolization methods in the literature.

Study	Method	CNT type	Size of airborne CNTs	CNT output Concentration	Remarks
Maynard et al. (2004)	A vortex shaker fluidized bed	SWCNT	Various sizes for different CNTs		Polydisperse particles
Lee et al. (2009)	A mechanical shaker	MWCNT	Mobility size peak ~ 200 – 300 nm, aerodynamic size peak ~ 2 urn	Concentration lower than the atomizing method in the same study	Concentration decreases rapidly at the initial stage
Lee et al. (2009)	An atomizer	MWCNT	Mobility size ~ 200 to 400 nm, aerodynamic size ~ 2 –3 μm	Total number concentration ~ 200 000/m^3 by SMPS *	Concentration decreases with time
Seto et al. (2010)	A Collison atomizer	MWCNT	Mobility size ~ 200 to 400 nm		
Mitchell et al. (2007)	A jet mill and cyclone	MWCNT	Mass median aerodynamic size ~ 0.7 to 2 μm, mobility size median ~ 350 to 400 nm	0.1 to 5 mg/m^3	High energy process to break up CNTs
Baron et al. (2008)	An acoustic feeder, knife-mill and cyclones	SWCNT	Mass size distribution peak ~ 4 μm	Up to 25 mg/m^3	Mass output efficiency 10%
McKinney et al. (2009)	An acoustic drum	MWCNT	Mass median aerodynamic diameter ~1.5 μm.	10 mg/m^3 for hours	Feedback control system for stable concentration
Myojo et al. (2009)	A Palas rotating brush generator with a two-component fluidized bed	MWCNT	Count median lengths ~ 4 to 6 μm under SEM	Number up to 20 000/cm^3, mass 4 mg/m^3 at a low feed rate	Concentration relatively stable
Ku & Kulkarni (2009)	An electrospray	SWCNT	Mobility size generally less than 500 nm, individual SWCNTs observed	Total particle number up to 27 000/cm^3	Ammonium acetate buffer solution used
Jennerjohn et al. (2010)	An electrospray	SWCNT MWCNT	Various sizes for different CNTs, SWCNTs in agglomerated form of the order of microns under TEM	Up to 0.18 mg/m^3	Output efficiency 9.4%
Kim et al. (2010)	An electrospray	MWCNT	Mobility size distribution with peaks around 150 and 400 nm, controllable agglomeration degree	Up to 2 mg/m^3	Ethanol used for CNT dispersion.

* SMPS: Scanning mobility particle sizer.

Table 2

Comparison of the primary particle size in diesel agglomerates measured by UNPA and TEM.

Engine load	Catalytic stripper usage	Primary particle sizes from UNPA (nm)	Primary particle size from TEM (nm)
Light	No	30.1	
Light	Yes	29.5	23.2 ± 6.6
Heavy	No	24.7	
Heavy	Yes	24.2	23.9 ± 6.8